

# Linköping University Post Print

## ZnO nanoparticles or ZnO films: A comparison of the gas sensing capabilities

Jens Eriksson, Volodymyr Khranovskyy, Fredrik Söderlind, Per-Olov Käll, Rositsa Yakimova and Anita Lloyd-Spets

N.B.: When citing this work, cite the original article.

### Original Publication:

Jens Eriksson, Volodymyr Khranovskyy, Fredrik Söderlind, Per-Olov Käll, Rositsa Yakimova and Anita Lloyd-Spets, ZnO nanoparticles or ZnO films: A comparison of the gas sensing capabilities, 2009, Sensors and actuators. B, Chemical, (137), 1, 94-102.

<http://dx.doi.org/10.1016/j.snb.2008.10.072>

Copyright: Elsevier Science B.V., Amsterdam.

<http://www.elsevier.com/>

Postprint available at: Linköping University Electronic Press

<http://urn.kb.se/resolve?urn=urn:nbn:se:liu:diva-17603>

# **ZnO nanoparticles and ZnO films, a comparison of the gas sensing capabilities**

Jens Eriksson, Volodymyr Khranovskyy, Fredrik Söderlind, Per-Olov Käll, Rositza Yakimova, Anita Lloyd Spetz

Department of Physics, Chemistry and Biology (IFM), Linköping University, SE-581 83 Linköping, Sweden, [jenser@ifm.liu.se](mailto:jenser@ifm.liu.se) / [jens.eriksson@imm.cnr.it](mailto:jens.eriksson@imm.cnr.it)

## **Abstract**

Zinc oxide is an interesting material for bio and chemical sensors. It is a semiconducting metal oxide with potential as an integrated multisensing sensor platform, which simultaneously detects parameters like change in field effect, mass and surface resistivity. In this investigation we have used resistive sensor measurements with respect to oxygen sensitivity in order to characterize sensing layers based on electrochemically produced ZnO nanoparticles and PE-MOCVD grown ZnO films. Proper annealing procedures were developed in order to get stable sensing properties and the oxygen sensitivity towards operation temperature was investigated. The ZnO nanoparticles showed a considerably increased response to oxygen as compared to the films. Preliminary investigations were also performed regarding the response to other gases present in car exhausts or flue gases.

*Keywords:* Zinc oxide, nanoparticles, multisensing, gas sensor.

# 1. Introduction

Chemical sensors with metal oxides as sensing material have been around for a long time as a low cost alternative for gas detection devices. However, they have, to some extent, suffered from limitations in sensitivity, selectivity and stability when compared to more expensive alternatives. Recent advances in nanotechnology and nanomaterials have fostered fabrication techniques that can be harnessed to increase the response and performance of these materials [1, 2]. This is because their performance is governed by the exposed surface area; the gas sensing mechanism being due to reactions that occur at the sensor surface. Fabrication methods, which increase the active surface area will thus have a considerable effect on the sensor performance.

Many recent reports have shown that by carefully controlling the nanostructure of metal oxide sensing layers greatly improved sensing properties can be achieved. Rella et al. showed that SnO<sub>2</sub> films yielded a better response to NO<sub>2</sub> and CO when the grain size was kept below 10 nm [3]. Yamazoe and Shimano have studied the role of shape and size of nanocrystals for the response to oxygen of semiconducting materials [4]. Growth of nanowires, nanorods and nanobelts has demonstrated that the high surface to volume ratio gave these nanostructures enhanced sensor qualities [2, 5]. The most common methods to produce sensing layers require thermal treatment of the film, which, unfortunately, causes grain growth and has a detrimental effect on the surface to volume ratio of the sensing layer [6]. Nanostructures, like nanorods or nanoparticles, that exhibit a high degree of crystallinity suffer less from this drawback and should enable production of sensor devices with good long-term stability [2, 7, 8]. A multitude of metal oxides can potentially be used for these types of sensors, including tin, indium, titanium and zinc oxides. The metal oxide surfaces of these materials also exhibit

good long-term stability while operating under physiological conditions [9]. Other examples of well established sensor technologies, which recently have benefitted from nanotechnology implemented in sensing layers are field effect sensors [10] and quartz crystal microbalance, QCM, sensors [11].

ZnO is an interesting material for bio and chemical sensors since it is a semiconductor with a band gap of 3.4 eV and has an oxygen containing surface. Field effect transistor (FET) devices based on silicon or silicon carbide require the growth of an oxide, such as silicon dioxide, to serve as gas sensors [12]. Gas sensing of e.g. reducing gases like hydrogen, ammonia and hydrocarbons on these Si- or SiC-FET devices involves dissociation of the molecules on a catalytic metal and adsorption of hydrogen on oxygen atoms on the silicon dioxide surface forming OH groups [13]. The OH groups are strong dipoles on the oxide surface of FET devices and are detected through the electric field induced in the insulator, which changes the electrical characteristics of the transistor. The most attractive properties of ZnO as a sensing material is its multisensing mechanisms for gases. It can be operated as a FET gas sensor, a resonator because of its piezoelectric properties and as resistivity sensor. Furthermore, we have previously taken advantage of the oxygen atoms present in the surface of the ZnO when we performed successful functionalization of the ZnO with biomolecules as a step towards a multifunctional transducer for biosensor devices [14, 15].

In view of this, we report here a study of the oxygen sensing capabilities of different types of ZnO layers with the main focus being to investigate the influence of surface morphology on the gas sensing capabilities. The purpose of this study is not to fabricate an oxygen sensor, but rather to use the oxygen sensing capabilities of different sensing layers as a means to evaluate their sensing characteristics and to further add to the understanding of these materials.

Comparison of the gas sensing properties have been performed for different size and shape of nanostructures, as described earlier in this section [2-5]. Here we compare the gas sensing behaviour of films and nanoparticles, which we think are of fundamental interest. The gas sensing capabilities of polycrystalline ZnO thin films have thus been compared to those of layers comprising electrochemically produced ZnO nanoparticles with a high degree of crystallinity. The high crystallinity of the nanoparticles should allow for devices with good long term stability. These films were deposited on top of SiC/SiO<sub>2</sub> structures. Changes in resistance, in response to variations in gas concentration, have been measured in order to characterize the materials by their optimal operating temperature, sensitivity, stability and reversibility of the response.

## **2. Experimental**

### **2.1 Samples**

Figure 1 a and b shows a schematic illustration of the two types of structures that have been investigated in this study. Both types of sensors consisted of a ZnO layer deposited on top of a SiC/SiO<sub>2</sub> structure. The purpose of the SiO<sub>2</sub> layer was to make sure that any change in resistance detected between the contacts originates from resistance variations in the film being studied, and not the underlying SiC. The only difference between the two structures was that for the films the contacts are added on top of the ZnO layer, while for the nanoparticles the contacts are deposited directly on top of the SiO<sub>2</sub> layer. The contacts for measuring resistance, were made by either thermal evaporation or sputtering of a bilayer of Ti/ Pt or Au (10/ 300 nm) through a shadow mask. Prior to deposition, the surface was cleaned and sonicated in acetone for 10 min, followed by 10 min of UV/ozone treatment to remove organic contaminants. Contact distances ranging from 200 μm – 2 mm have been studied. The

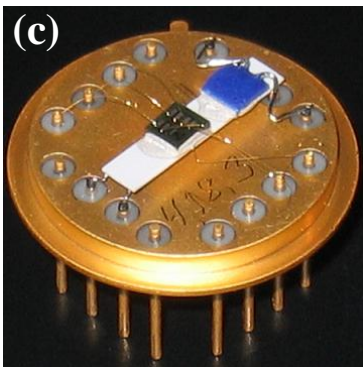
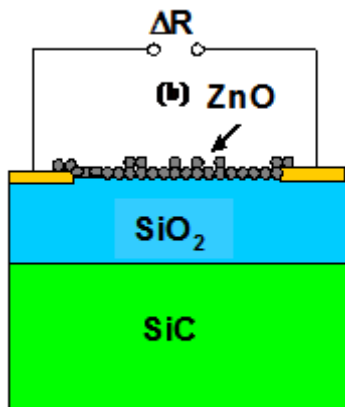
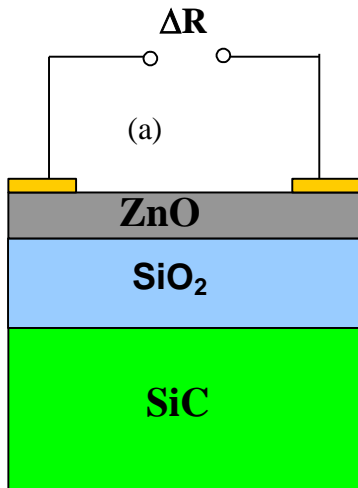


Fig. 1. Schematic view of a SiC/SiO<sub>2</sub> device with (a) a film of PE-MOCVD grown ZnO (b) a ZnO nanoparticle layer (c) a mounted sample glued to a ceramic heater, the blue device is a temperature sensor, (a so called Pt 100 element, that is a Pt resistor of 100 Ohm at room temperature). Bonding wires connect the contacts of the sample to the pins in the holder

SiC/SiO<sub>2</sub> structures were manufactured by thermal oxidation of 4H-SiC, which yielded 30 nm of SiO<sub>2</sub>. This was followed by deposition of an LPCVD nitride layer, which is subsequently reoxidized, resulting in a top SiO<sub>2</sub> layer of about 50 nm, and a total insulator thickness of about 80 nm.

## **2.2 ZnO thin film fabrication**

The ZnO films were prepared by the PEMOCVD (plasma enhanced metalorganic chemical vapour deposition) technique on SiC/SiO<sub>2</sub> substrates. PEMOCVD has been previously suggested as one of the most suitable techniques for low-temperature, high-quality deposition of ZnO thin films using low cost and non-toxic metalorganic precursors, here acetylacetonate (Zn(Acac)<sub>2</sub>). For more details, please see [16, 17]. Before deposition, the substrates were cleaned in acetone (10 min) and ethanol (10 min), then rinsed in deionized water and blow-dried with nitrogen. Recently we have investigated the structural, morphological, electrical and optical properties of pure ZnO films deposited over a wide temperature range on different substrates [18]. Scanning electron microscopy (SEM) was used to reveal the uniformity of the films and quality of the film/substrate interface (Leo 1550 Gemini SEM). The surface morphology was examined by atomic force microscopy (AFM - Veeco Digital Instruments Nanoscope 3100) in tapping mode. For the films in this study the substrate temperature was  $T_{\text{sub}} = 350^{\circ}\text{C}$ , which promotes the columnar growth of the polycrystalline film with a characteristic grain size of  $\approx 35 \pm 15$  nm, and a surface root means square roughness  $R_q = 1.5 \pm 0.5$  nm [19]. The total layer thickness was  $\approx 250 \pm 30$  nm.

### **2.3 Nanoparticle synthesis - EDOC**

Electrochemical deposition under oxidising conditions, EDOC, is an efficient method for the synthesis of nanocrystalline metal oxide particles. When properly controlled, it yields well-defined synthesis products with narrow particle size distributions and a high degree of crystallinity [20]. In the case of ZnO particles the anode in the electrochemical cell, from which the oxide particles are to be formed, is made of zinc. An organic solvent, 2-propanol (Scharlau. Chemie S.A), together with a quaternary ammonium salt, TBAB (tetrabutylammonium bromide, Fluka) are used as electrolyte. The ammonium salt acts both as a medium for current transport and as capping molecules for the nanoparticles formed. The metal ions migrated to the inert stainless steel cathode, where reduction and formation of metal particles occur. To render the particles soluble in a non-polar solvent 1.25 ml of oleic acid (KEBO AB) was added as a capping agent. Bubbling air into the solution causes immediate oxidation of the particles. The particle size could be controlled by the current density at the cathode. Lower currents yield larger particles and vice versa. Here the current density at the cathode was kept at  $1.5 \text{ mA/cm}^2$ . More details can be found in Ref. [10].

The product solution containing the nanoparticles was drop deposited onto the SiC/SiO<sub>2</sub> devices by means of a 0.5  $\mu\text{l}$  micropipette in order to produce sensing layers of nanoparticles. The volumes applied were 0.5 – 2  $\mu\text{l}$ . The devices were subsequently heated as described in section 4.1.2. in order to remove the organic capping material.

The size and crystallinity of the nanoparticles were studied by both x-ray powder diffraction (Philips APD powder diffractometer, CuK $\alpha$  radiation) and transmission electron microscopy (FEI Tecnai G2 operated at 200 kV). The effects of the annealing procedure were characterized by thermogravimetric analysis.

## **2.4 Sensor mounting**

The sensor structure was glued onto a ceramic heater together with a temperature sensor for temperature control. The contacts of the heater and the temperature sensor were welded to the pins of a 16 pin header. Electric contacts were made from the sensor to the pins with gold wire bonding. A mounted sensor device is shown in Fig. 1 (c). During measurements the sensor was enclosed in an aluminum flow cell, having a 1 cm<sup>3</sup> headspace over the sensors, through which the gas was carried across the sensor surface. During the measurements the flow cell was connected to a box with all the necessary electronics for measuring resistance as well as measuring and controlling the temperature of the sensor devices.

## **2.5 Gas sensitivity measurements**

Gas sensing measurements were conducted under laboratory conditions, using an in-house gas mixing system that comprised mass flow controllers (Bronkhurst High-tech B.V Netherlands, model F-201C-RA-11-V 100 and 20 ml/min). Sensing characteristics in terms of sensor signal, response and sensitivity [21] were studied through the detection of oxygen concentrations ranging from 1 to 100% oxygen in a background of nitrogen, maintaining close to atmospheric pressure and a constant total flow of 100 ml / min. The temperature of the films was varied from 150 to 550°C. The resistance was measured using a Keithley 2000 multimeter configured in the two wire mode.

The response is defined as

$$R = \frac{R_g}{R_{N_2}} \quad (1)$$

Where  $R_g$  is the resistance under test gas exposure and  $R_{N_2}$  is the resistance in the nitrogen carrier gas in the absence of test gas.

The sensors were exposed to O<sub>2</sub> pulses to test the sensitivity of different sensing layers. Two types of O<sub>2</sub> test procedures were performed, one for ‘low’ and one for ‘high’ concentrations. The low concentration test procedure was as follows: the O<sub>2</sub> concentration was varied in two ways, 1, 2, 3, 4, 5, and 8 % O<sub>2</sub> in N<sub>2</sub>, each pulse lasted for 5 minutes and pulses were separated in time by 60 minutes in the carrier gas, or steps of 1 % from 1 to 10 and then back to 1 % again, in 5 minute pulses with 10 minutes between pulses. For high concentrations the procedure was exactly the same except that the O<sub>2</sub> percentage was increased by a factor of 10.

The sensing layers yielding the best response to O<sub>2</sub> were also preliminary tested for response to 250 ppm of NH<sub>3</sub>, C<sub>3</sub>H<sub>6</sub>, H<sub>2</sub>, CO and NO. These measurements were performed in a background of 21% O<sub>2</sub> in N<sub>2</sub> (to simulate normal air conditions) with test pulses lasting for 5 minutes and with 60 minutes between each pulse.

The total flow rate was always kept at 100 ml/min.

### **3. Principle of operation and annealing procedures**

#### ***3.1 Sensing mechanism***

The electrical resistance of a metal oxide semiconductor changes in the presence of various gases. ZnO is a wide band gap semiconductor with excess metal ions, or oxygen vacancies that serve as electron donors (n-type). When ambient oxygen molecules adsorb on the ZnO surface they act as acceptors and ionize by taking up one or two electrons from the conduction

band and thus ionosorb as  $O^- / O^{2-}$ . This causes an electron depletion region to form in the material which increases the materials resistance [6, 22, 23].

In the presence of a reducing gas this process is reversed. The reducing gas reacts with the ionosorbed oxygen, releasing one or two electrons back into the conduction band and thus decreasing the resistance of the material.

### **3.2 Sensor operation**

Two processes are assumed to take place when ZnO is subjected to oxygen at elevated temperatures. One is diffusion into the bulk of the material and absorption at vacancy sites. Drift in the baseline, defined as the sensor signal in nitrogen, can be assigned to this process. The second process is adsorption on the surface of the material (which is responsible for the sensor response).

Figure 2 shows the sensor signal, that is, the resistance variation versus time of an unannealed film of polycrystalline ZnO during exposure to oxygen pulses from 1 to 10% at 500°C. In the beginning the resistance showed a rather high initial value which directly fell to a low value and then stayed below 1 MΩ. However, after about 200 minutes the sensor began to respond significantly to oxygen. A new baseline was subsequently reached at  $\approx 3$  MΩ. A possible explanation is that deep energy level sites, most likely bulk oxygen vacancies, were filled. Oxygen diffused into the bulk of the material in a non-reversible process and the diffusion depth was determined by the temperature. Once these deep energy level sites were filled, oxygen started to interact with the shallow energy level surface sites and thus the process was reversible after 200 min, as seen in Fig. 2. The behavior in Fig. 2 was not observed for the

ZnO nanoparticles, probably because they had to be annealed at  $> 500^{\circ}\text{C}$  before operation in order to remove the organic capping molecules.

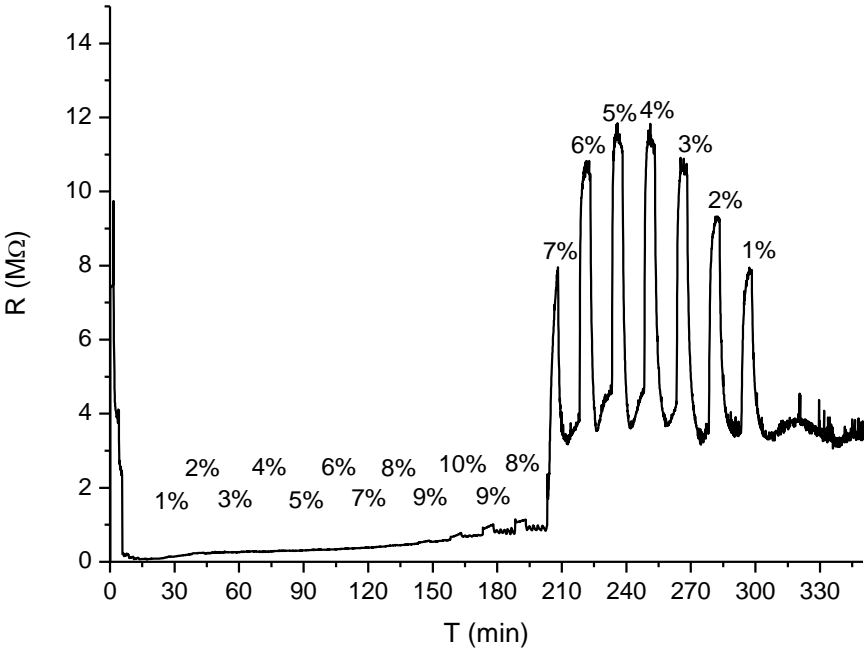


Fig. 2. Effects of annealing at  $500^{\circ}\text{C}$  of a ZnO film device in an ambiance of oxygen pulses(1-10%) with nitrogen as the carrier gas.

Depending on the material, the resistivity is determined by the barrier height at the grain boundaries for polycrystalline material or by the carrier concentration for single crystalline material. In both cases, a reduction of free charge carriers (through reduction of the O vacancies) will lead to an increase of the resistivity. In the sensor configuration used here we measure only surface resistivity. At a certain point of oxygen exposure the bulk absorption saturates and any change in resistance is now due only to surface adsorption, which is readily reversible as described above. When this point is reached the device can be operated as a gas sensor.

### ***3.3 Investigation of annealing procedures***

The resistance as a function of temperature showed different behavior during the initial measurements (oxygen pulses as described in 2.5) depending on the type of film and the annealing temperatures (in air) they had seen. The polycrystalline films behaved as a typical semiconductor; increasing the temperature reduced the resistance, and the reduction begins to saturate as the temperature got sufficiently high. Grain growth at elevated temperature caused some hysteresis effect when going back down in temperature.

For the particles, annealing at temperatures  $\geq 520^{\circ}\text{C}$  was necessary. When testing particles initially annealed at  $< 500^{\circ}\text{C}$  at temperatures above  $500^{\circ}\text{C}$ , the first oxygen pulse larger than  $\approx 10\%$  caused a dramatic, sudden, irreversible and for the gas sensing properties detrimental reduction of the resistance. This could be due to charring of organic material remaining after insufficient annealing. Particles annealed at  $\geq 520^{\circ}\text{C}$  did not exhibit this reaction. Their  $R(T)$  behaviour still differed from that of the polycrystalline films when going back down in temperature. For the films the resistance was permanently increased, whereas for the high temperature annealed particles it was permanently reduced. To better understand the difference between nanoparticles annealed at different temperatures, thermogravimetric analysis was performed.

## 4 Results

### 4.1 Characterization of sensing layers

#### 4.1.1 Thermogravimetric analysis

To obtain films of ZnO nanoparticles the organic material (oleic acid) added in the synthesis has to be removed by an appropriate heat treatment. Furthermore, in order to minimize the particle agglomeration induced by annealing, the temperature should not be too high. Figure 3 shows thermogravimetric analysis curves for samples heated from room temperature up to 600°C, with a temperature increase rate of 20°C/min. These samples were prepared through drop deposition of 22 µl of the as produced ZnO nanoparticles in solution (toluene) onto 7 x 7 mm<sup>2</sup> Si/SiO<sub>2</sub> tablets.

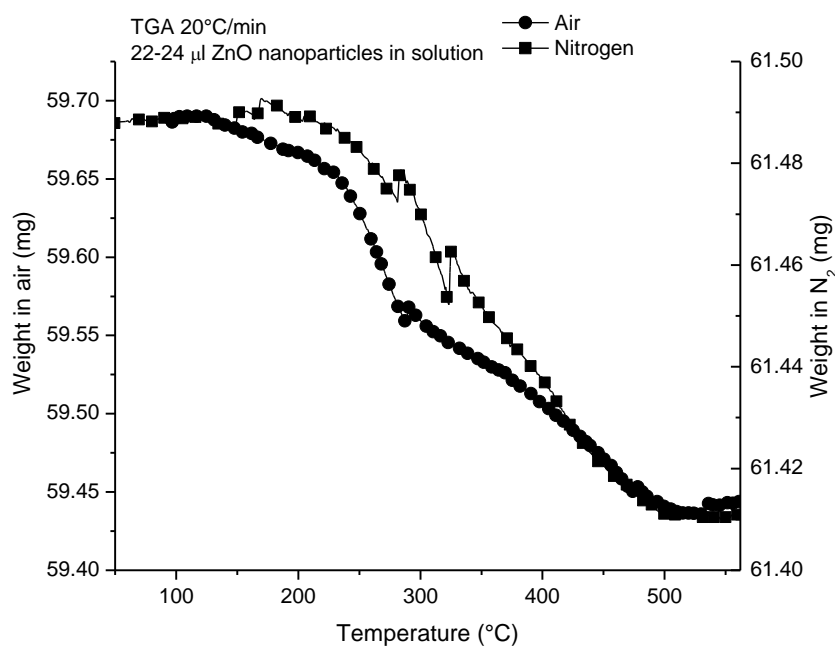


Fig. 3. Thermogravimetric analysis, TGA, in air or N<sub>2</sub> ambience, respectively, from room temperature up to 600°C, with a temperature increase rate of 20°C/min. The spikes seen around 300°C are artefacts due to residues from earlier measurements dropping down on the sample during the measurement.

The TGA curves show that there were several different processes contributing to the complete dissipation of the organic material. The first process appears to start at  $\approx 120^\circ\text{C}$ , and the fact that it was present in both curves hints towards it being pyrolysis. It was probably due to the destruction of the ester bond between the oleic acid surface OH groups, resulting in a release of  $\text{CO}_2$  (this has not been confirmed). A second process apparent between  $250^\circ\text{C}$  and  $500^\circ\text{C}$  was likely due to the decomposition of hydrocarbons in the oleic acid. Both curves indicate that the oleic acid was completely removed at about  $500^\circ\text{C}$ . This may explain the behavior described in section 3.3 for the nanoparticle material. The oleic acid had not been completely removed, and so exposure to oxygen at temperatures above  $500^\circ\text{C}$  caused the remaining organic material to char instead of decomposing as it would during the slow increase of the temperature during annealing.

Initially the films were only annealed up to  $500^\circ\text{C}$ . However, sensors fitted with such layers did not work well, for the reason discussed above. When the annealing temperature was raised to  $520$  or  $550^\circ\text{C}$  the sensing capabilities increased significantly, indicating that  $520^\circ\text{C}$  was enough to remove all of the oleic acid. Interestingly, the films annealed at  $550^\circ\text{C}$  were significantly less sensitive than those annealed at  $520^\circ\text{C}$ . The inferior sensitivity of the former could be due to agglomeration of the particles, reducing the surface to volume ratio, which in turn reduces the sensitivity. SEM studies, as reported in section 4.1.1, confirmed the agglomeration. A further possibility is that the change in resistivity was partly due to a phase transition of ZnO taking place in certain temperature regions but no such transition was observed in XRD studies.

Based on these findings in sections 3.2 - 4, annealing of both nanoparticle and polycrystalline film based devices, in this study was performed in air up to 520°C. The heating schedule was a heating rate of 2°/ min with 1 h holding periods at 350, 450 and 520°C.

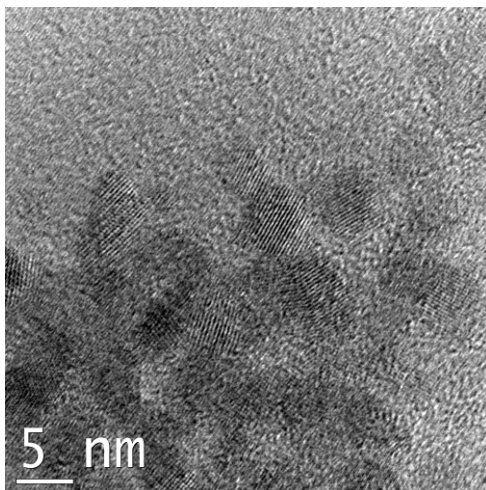
#### **4.1.2 SEM, TEM and AFM imaging.**

As seen in the TEM image in Fig. 4 (a), the as-synthesized nanoparticles were about 5 nm in diameter. This is in agreement with what has been previously reported [25, 26]. SEM images of samples annealed at 450°C, see Fig. 4 (b), showed particle growth to some extent. For an annealing at 550°C, see Fig. 5 (c), the particles aggregated and grew from about 5 to 50-100 nm. This was consistent with the results of Berber et al. [20] who reported a growth in ZnO particle size from 8 to 80 nm after annealing at 550°C.

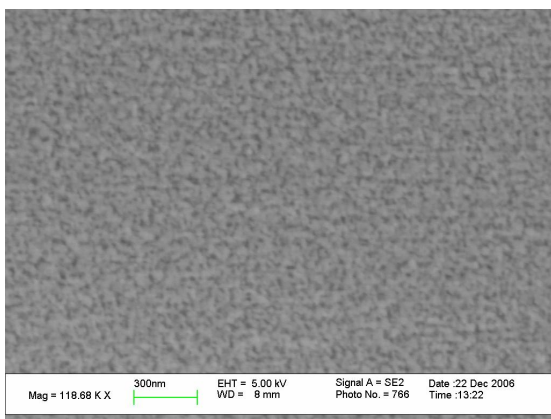
For the analysis of ZnO films, the SEM profile, see Fig. 5 (a), showed columnar structure resulting in a nanostructured surface topography revealed in an AFM image, see Fig. 5 (b).

#### **4.1.3 X-ray diffraction spectroscopy.**

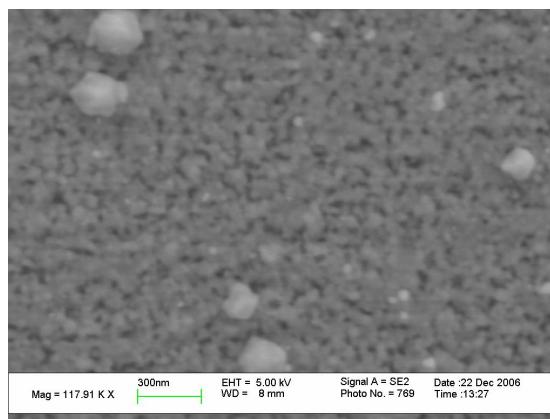
Figure 6 shows X-ray diffractograms for ZnO nanoparticles following different heat treatments (as-prepared, 200°C, 400°C and 600°C). The as-prepared nanoparticles were only ~5 nm in diameter (as observed by TEM) resulting in very broad diffraction peaks of low intensities. As the annealing temperature was increased, the crystals grew, producing the well-defined hexagonal ZnO diffraction pattern.



(a)

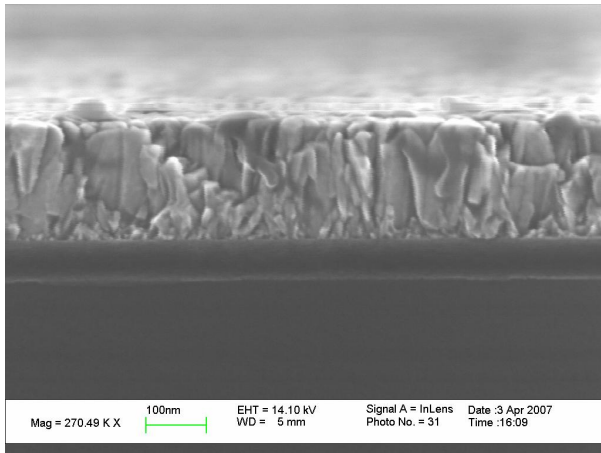


(b)

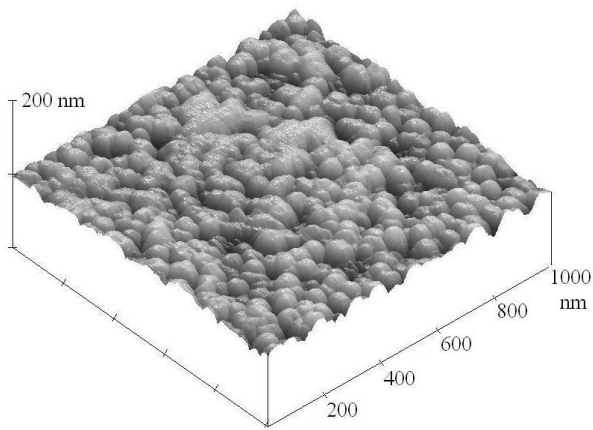


(c)

*Fig. 4 (a). Plan view TEM image of as produced ZnO nanoparticles (dark areas represent particles) and SEM images of nanoparticles (light areas) annealed up to (b) 450°C and (c) 550°C.*



(a)



(b)

Fig. 5. Cross sectional SEM image of a polycrystalline ZnO/SiO<sub>2</sub>/SiC sample (a) and AFM images of the sample surface (b).

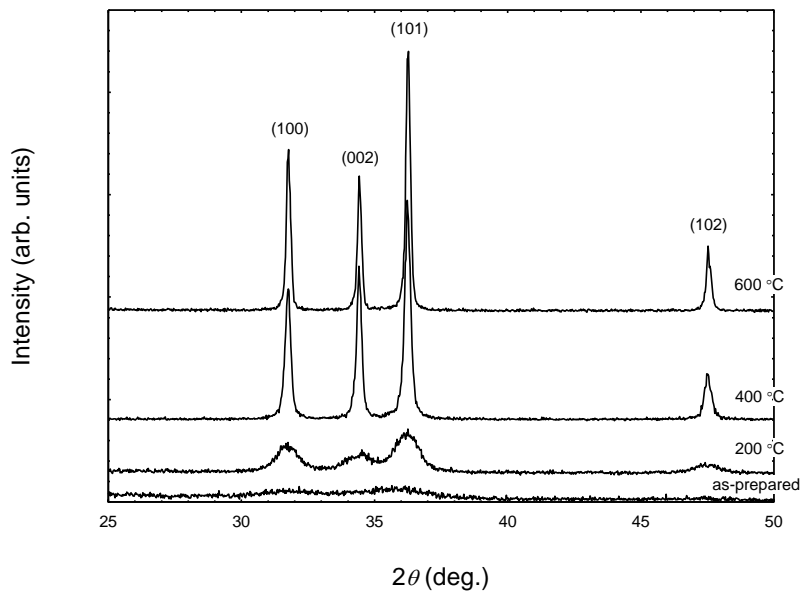


Fig. 6. X-ray diffractograms of as-prepared ZnO nanoparticles and nanoparticles that have been heat treated at 200°C, 400°C and 600°C, for 14 h at each temperature.

## 4.2 Gas response

### 4.2.1 Nanoparticles

Eleven sensors with sensing layers of nanoparticles were tested. Variations in film thickness (actual thickness was not measured, but three different solution volumes, 0.5, 1.0 and 2.0  $\mu\text{l}$ , were applied) and inter-electrode (contact) distance (200-2000  $\mu\text{m}$ ) did not appear to affect the sensitivity. However, a smaller contact distance was found preferable since the resistance for sensors with a larger contact separation was too high to be measured at temperatures lower than  $\approx 400^\circ\text{C}$ . The nanoparticle samples that had been annealed at sufficiently high temperatures ( $520^\circ\text{C}$ , procedure described in section 3.4) showed a reversible response to oxygen over the range of 1-80% at temperatures ranging from 250- to  $550^\circ\text{C}$ . Overall, the nanoparticle samples were considerably more stable than the samples based on films. After some initial drift they usually levelled out and maintained a stable baseline. Fig. 7 shows the signal of a very stable sensor.

Fig. 8 shows the sensor signal for a sample with nanoparticles (contacts separated by 200  $\mu\text{m}$ , 0.5  $\mu\text{l}$  ZnO nanoparticles), annealed at  $520^\circ\text{C}$ . The sample was exposed to oxygen pulses, varying in concentration from 1 to 8%, in steps of 1% and with nitrogen as a carrier gas, at  $450^\circ\text{C}$ , see Fig. 8 (a) and at  $550^\circ\text{C}$ , see Fig. 8 (b). After some initial drift during the first hour of testing (not shown in the figure), the sensor reached a stable baseline. A comparison of the results from measurements at 450 and  $550^\circ\text{C}$  suggests that there was a trade-off between sensitivity and drift / response / relaxation time. At  $450^\circ\text{C}$  the response was higher but the relaxation time was longer. Using  $\tau_{\text{res}}$  as the time it took to reach 90% of the full response, and  $\tau_{\text{rec}}$  as the time it took for the signal to recover to within 10% of its original baseline,  $\tau_{\text{res}} > 5$  and  $\tau_{\text{rec}} \approx 16,5$  min at  $450^\circ\text{C}$ , while  $\tau_{\text{res}} \approx 1$  and  $\tau_{\text{rec}} \approx 2,5$  min at  $550^\circ\text{C}$ . Thus, too fast

variations in oxygen concentration at 450°C induced a drift in the baseline. The speed of response was significantly higher at 550°C and the drift was thus reduced, however, at the cost of a reduced response as shown in Fig. 8 (b).

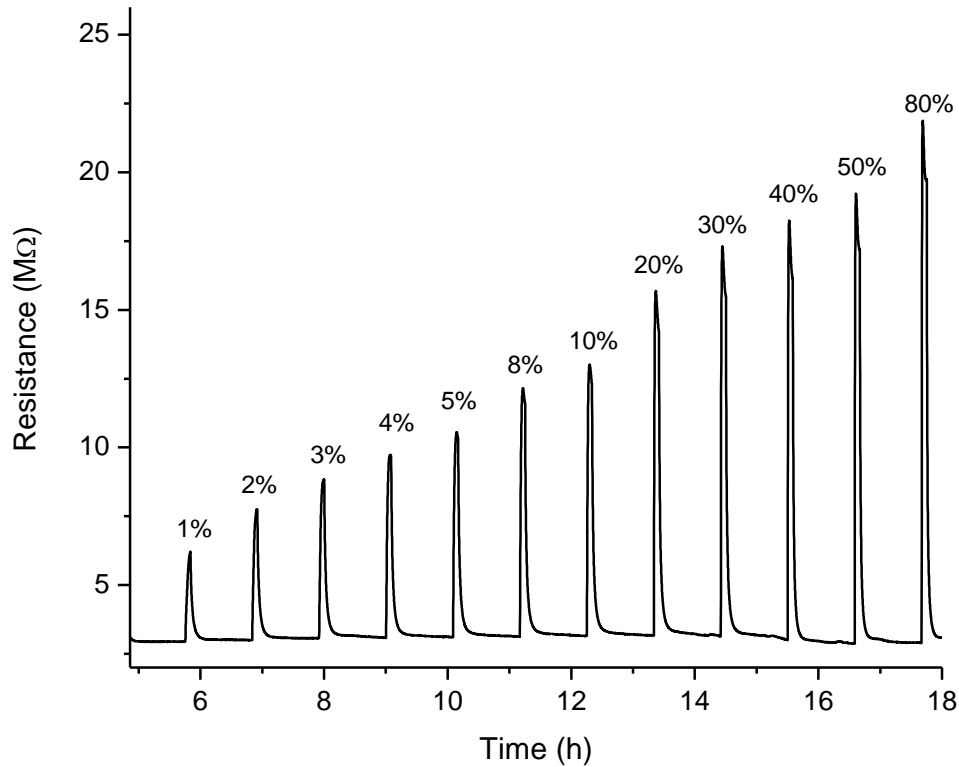
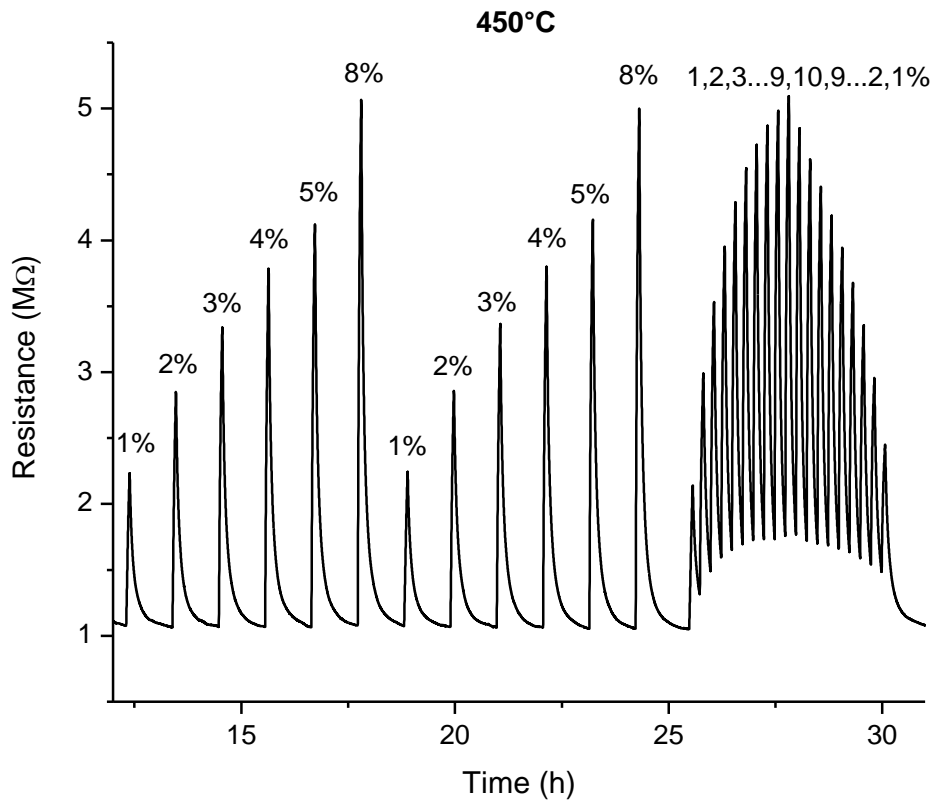
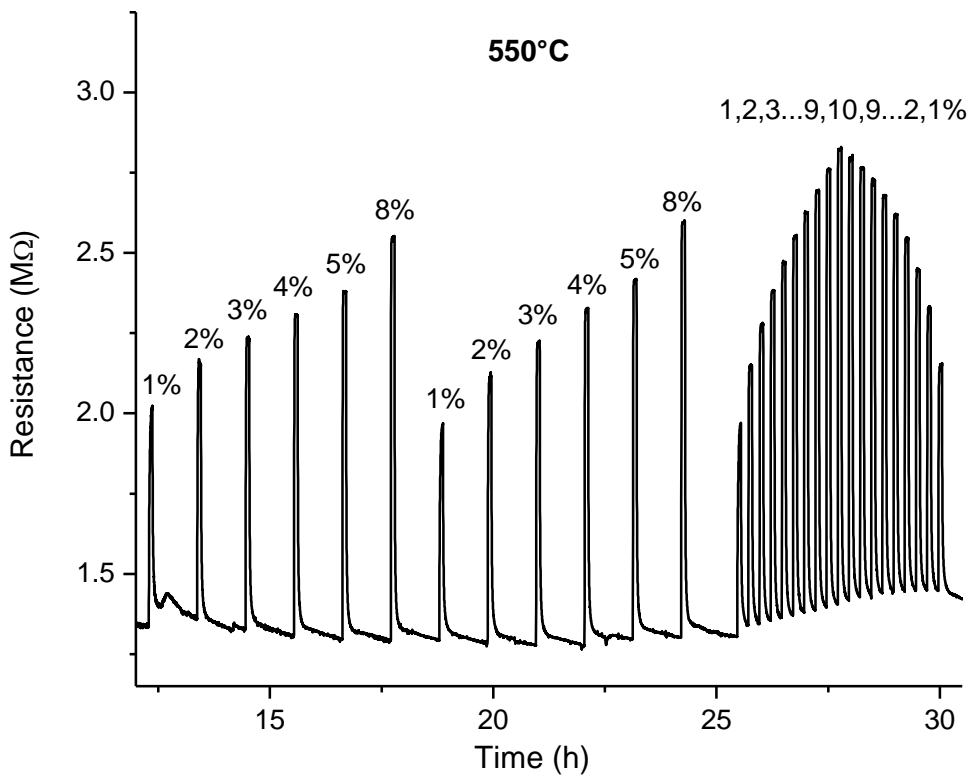


Fig. 7. Resistive sensor signal versus time for ZnO nanoparticles (1.0  $\mu\text{l}$  layer of nanoparticles and contact distance of 500  $\mu\text{m}$  in the finger electrode), annealed at 520°C, exposed to 1-80%  $\text{O}_2/\text{N}_2$  with  $\text{N}_2$  in between pulses at 450°C.

Fig. 9 shows the oxygen response ( $R_g/R_{\text{N}_2}$ ) for a sensor with nanoparticles at five different temperatures between 250 and 550°C. From 250°C up to 500°C the response steadily increased, while above this temperature (550°C) it rapidly and irreversibly decreased. Agglomeration of the ZnO nanoparticles at 550°C was most likely the reason for the decrease in oxygen sensitivity at this temperature, as discussed in 3.3 and studied in 4.1.



(a)



(b)

*Fig. 8. Resistive sensor signal versus time of ZnO nanoparticles, initially annealed at 520°C, exposed to 1-8 % oxygen at (a) 450 and (b) 550°C.*

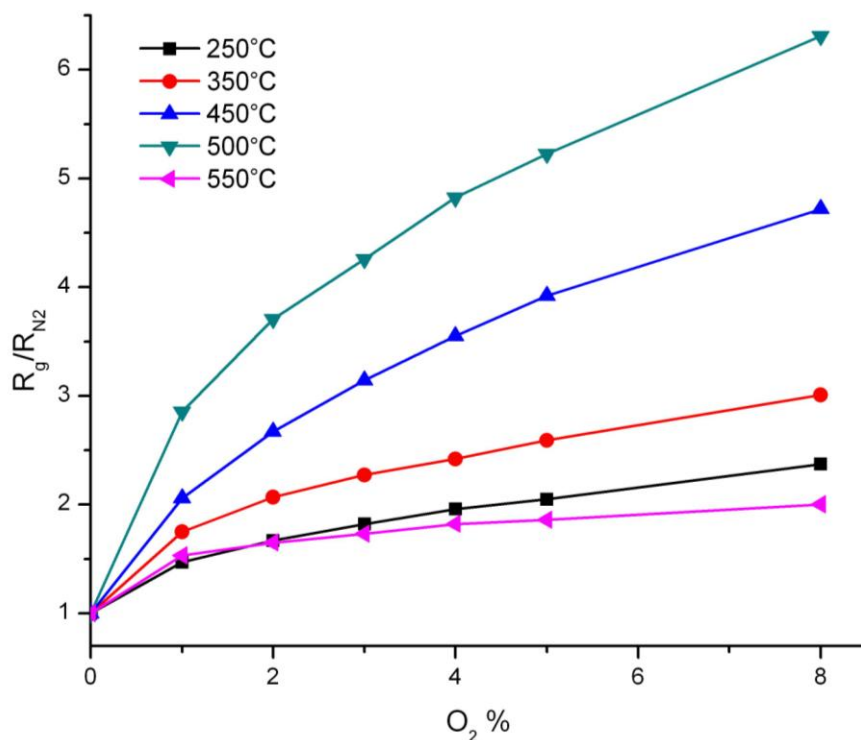


Fig. 9. The sensor response,  $R_g/R_{N_2}$ , versus  $O_2$  concentration for nanoparticles at four different temperatures from 250 to 550°C, in the slow measurement mode.

#### 4.2.2 Polycrystalline films

The polycrystalline films exhibited an overall lower response than the particles. They were also less stable, with a drifting and often rather noisy baseline. The baseline drift sometimes fluctuated and for some samples did not reach a stable value. At 500°C the polycrystalline films needed  $\approx 12$  hours to reach a stable baseline, which may have been shorter for a higher annealing temperature. Another problem encountered with the films was that exposure to high oxygen concentrations seemed to reduce the sensitivity in subsequent measurements at lower concentrations.

Fig. 10 shows the signal of a sensor with a polycrystalline film operated at 450°C, after initial annealing at 550°C during exposure to oxygen concentrations from 1-80%. Compared to a

similar test for a sensing layer of particles shown in Fig. 7, the baseline was significantly noisier, exhibited a bit more drift and the response was lower.

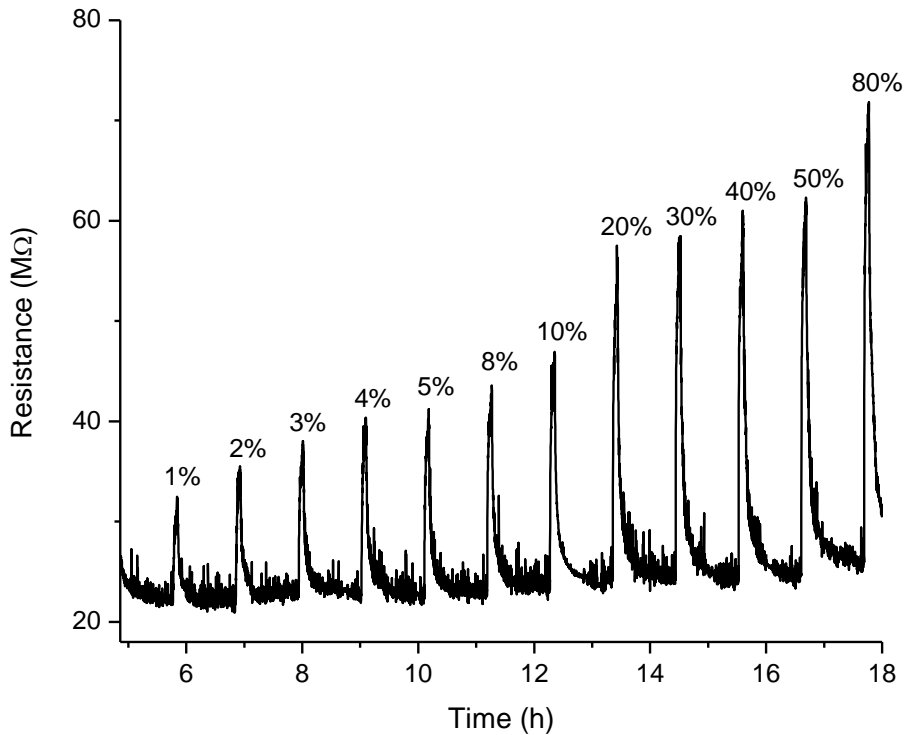


Fig. 10. Resistive sensor signal versus time for a polycrystalline film exposed to 1-80%  $O_2$  at  $450^\circ C$ .

#### 4.2.3 Oxygen sensitivity

Illustrated in Fig. 11 (a) and (b) is a comparison of the  $O_2$  response,  $R_g / R_{N_2}$ , versus oxygen partial pressure in oxygen / nitrogen gas mixtures (total pressure  $\approx 1$  atm) of films versus particles at  $450$  and  $500^\circ C$ , for the samples that gave the highest response in their respective category. Both the response and the sensitivity, of which the latter is the slope of the response versus oxygen concentration curve [21] was significantly higher for the nanoparticles as compared to the devices based on ZnO films. The marked data points in Fig. 11 (a) and (b) represent the experimentally measured signal and the solid curves the fitted Langmuir isotherm for dissociative adsorption. Dissociative  $O_2$  adsorption on ZnO is suggested already from the equilibrium equation and in Ref. [26]:

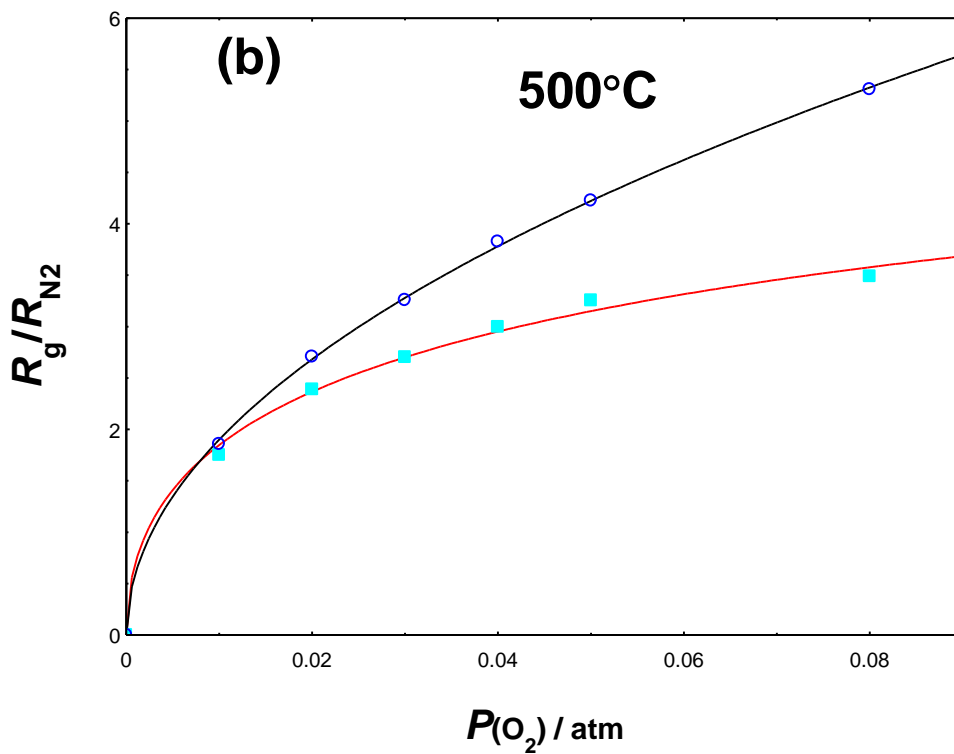
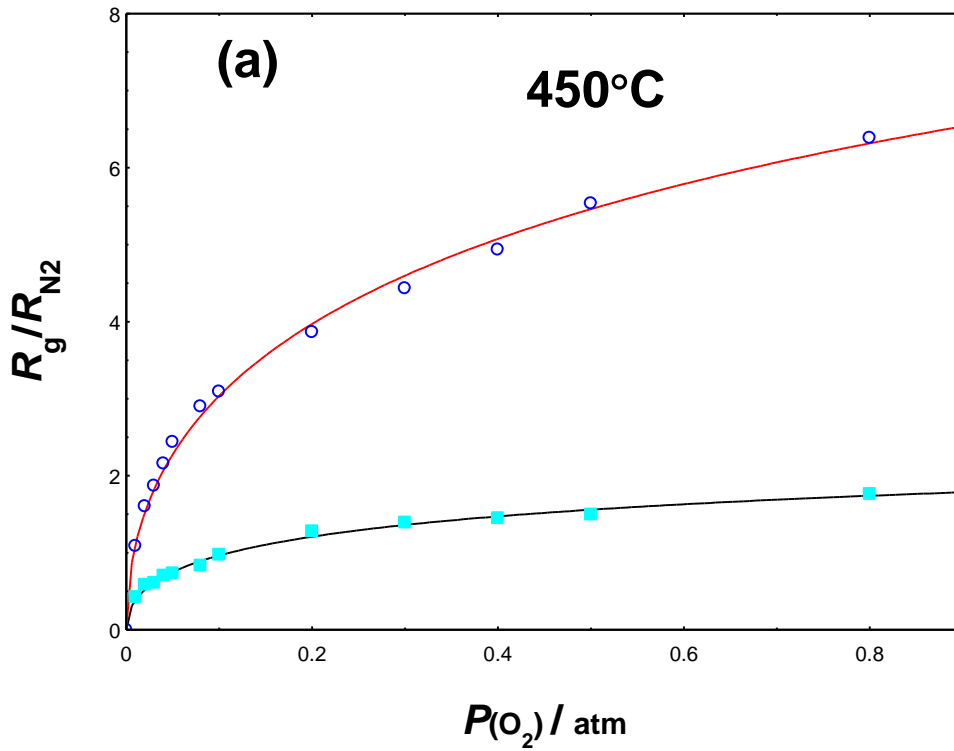
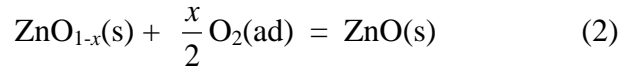


Fig. 11. Response versus  $O_2$  concentration for ZnO film and ZnO nanoparticles from (a) 1-80% at 450°C (b) 1-8% at 500 °C (circles: nanoparticles, squares: ZnO film). The lines represent Langmuir plot fits.



Assuming the measured signal is proportional to  $\theta$ , the fractional coverage of the surface sites available for oxygen adsorption, i.e.  $R_g / R_{N_2} = \alpha\theta$  with  $0 \leq \theta \leq 1$ , the Langmuir isotherm can be expressed as

$$\frac{R_g}{R_{N_2}} = \frac{\alpha\sqrt{Kp}}{1 + \sqrt{Kp}} \quad (3)$$

In Eq. (3)  $\alpha$  is a scale constant representing the (theoretical) maximum value for the response, i.e. for a saturated system for which  $\theta \approx 1$ . The constant  $K$  is the ratio between the rate constants for oxygen adsorption,  $k_a$ , and desorption,  $k_d$  ( $K = k_a/k_d$ ), respectively, and  $p$  is the oxygen partial pressure. The least squares values obtained for  $\alpha$  and  $K$  for the ZnO film and nanoparticles at 450°C and 500°C are given in Table 1.

Table 1. Constants in the Langmuir isotherm in Eq (3).

450 °C		
	ZnO film	ZnO nanoparticles
$\alpha$	3.11	15.4
$K$	2.03	0.603
500 °C		
$\alpha$	7.33	369
$K$	11.4	$2.68 \cdot 10^{-3}$

As seen in Figs. 11 (a) and (b) and in Table 1, the measured response versus pressure was higher at 500°C than at 450°C, corresponding to higher  $\alpha$  values for both film and particles at the former temperature. Also, the  $\alpha$  values were considerably larger for the particles than those for the film at both temperatures. (Note in Fig. 11 (b) that at 500°C the response was measured only up to  $P = 0.08$  atm.) In addition, while for the film the rate constant for adsorption was larger than that for desorption ( $K > 1$ ), the opposite is true for the particles ( $K < 1$ ). It is possible that states of lower energy are available in the surface region of the films, while these are not present in the nanoparticles, since the stoichiometry probably is closer to ideal. States of lower energy will result in faster adsorption as long as the diffusion is not a limiting factor, but also in longer desorption times. It would of course be interesting to test

also single crystalline ZnO films where a lower sensitivity may for example be compensated by better long term stability during high temperature operation.

#### **4.2.4 Response to other gases**

The response of a sensor device with ZnO nanoparticles to standard gas molecules like CO, NH<sub>3</sub>, NO, C<sub>3</sub>H<sub>6</sub> and H<sub>2</sub> present in car exhausts or flue gases was investigated at 450°C in a constant O<sub>2</sub> concentration of 21% (in N<sub>2</sub>), see Fig.12. This is a preliminary investigation. We have chosen a low concentration of the tested gases, 250 ppm, for which the response of the devices is not likely to saturate. The device responded significantly to all the gases tested, with the highest response level to propene and the response to NO in the opposite direction as compared to the other gases. It is interesting to note that the speed of response was much faster for these gases as evidenced from a comparison to the speed of response to oxygen, compare Figs 8 (a), 10 and 12. This suggests the possibility of different sensing mechanisms for oxygen and other gaseous species. It is likely that the reducing gases interact with adsorbed oxygen on the sensor surface [27]. Reducing gas molecules, which react with adsorbed oxygen ions will become oxidized, while the oxygen ion gives back electrons to the ZnO surface and the resistivity of the sensor material will decrease, as seen in Fig. 12. An exception here was the response to NH<sub>3</sub> in Fig. 12, where the sensor did not return to the base line in between the exposures. This also seemed to affect to some extent the response to the following NO pulses. In order to get a total picture of the response pattern of the ZnO nanoparticle sensor this investigation should be performed for different concentrations and at different temperatures, and it is especially interesting to study if the other gases also give a Langmuir response. Furthermore, e.g. DRIFT (Diffuse Reflectance Transform Infrared) spectroscopy should be used in order to reveal the adsorbed species on the sensor surface during gas exposure at different temperatures [13, 28]. However, the main interest in this

paper was the comparison between sensors based on ZnO nanoparticles and films. Since the nanoparticles have shown to be the superior sensor material of the two, these preliminary investigations of the response to other gases were performed with nanoparticles as the sensing layer. In future studies a comparison of the gas response between sensors with nanoparticles of different size would be interesting in order to further elucidate the particle size effect. Preliminary results have shown that doping by e.g. Ga yield ZnO sensing layers interesting to study regarding gas sensitivity to e.g. NO<sub>2</sub> [29]. In the future we will also produce devices for field effect measurements on ZnO with multifunctional sensor devices as the goal. Preliminary results of field effect measurements can be found in Ref. [14]

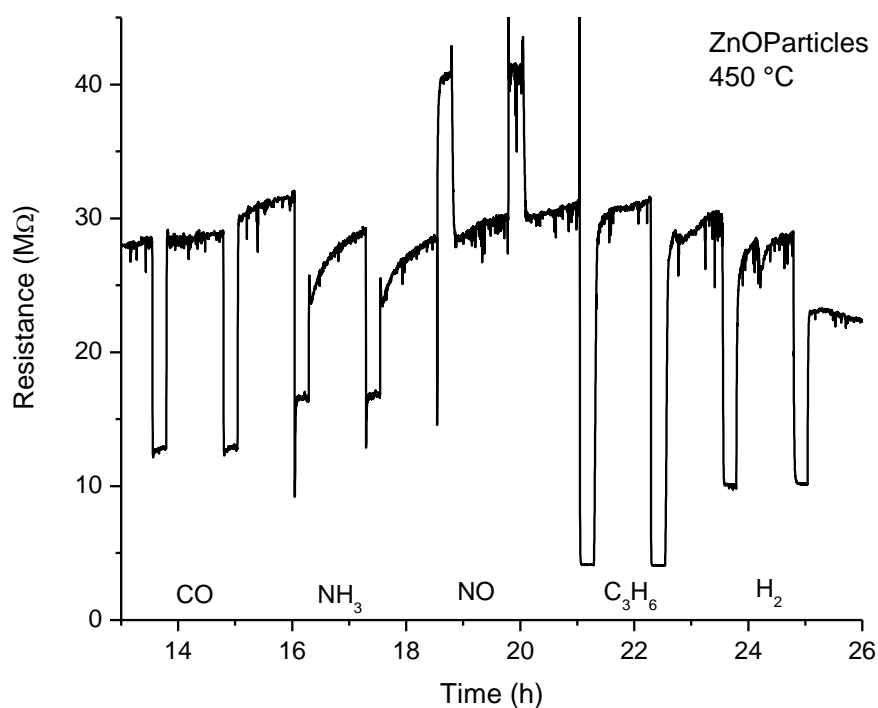


*Fig. 12. Response of ZnO nanoparticles to 250 ppm CO, NH<sub>3</sub>, NO, C<sub>3</sub>H<sub>6</sub> and H<sub>2</sub> (two pulses of each gas) at 450°C.*

## 5. Conclusions

Differently structured ZnO materials were characterized with respect to their interesting multiparameter sensing properties. The resistance change to oxygen in nitrogen was used to compare the sensing behavior of ZnO nanoparticles and ZnO films. We have shown that it was possible to use ZnO nanoparticles as sensing layers for chemical gas sensors, and that they exhibited higher sensitivity and stability than sensing layers of polycrystalline ZnO films. The higher sensitivity was ascribed to a larger surface to volume ratio, and the higher stability to the generally more stable single crystalline nanoparticles. The ZnO films tested here showed a columnar polycrystalline structure. Single crystalline films may have different properties. Annealing procedures for optimal stability and sensitivity were studied and established. The ZnO nanoparticles showed a reversible response to oxygen over a range of 1-80%, at temperatures ranging from 250 to 550°C. The optimal operating temperature, in terms of oxygen response, was found to be 500°C. The ZnO nanoparticles were also preliminary tested for reducing gases and found to be sensitive for NO, CO, propene and NH<sub>3</sub>, with the latter three exhibiting responses in the opposite direction as compared to oxygen.

## Acknowledgements

This work has been supported by the Swedish Research Council through two VR project grants and a Linné grant. One of the authors (V.K.) has been supported by the Swedish Institute and the IFM-Linné grant. Dr Robert Bjorklund is acknowledged for valuable comments on the manuscript.

## References

- [1] R.T. Rajendra Kumar, J. Grabowska, J.P. Mosnier, M.O. Henry, E. McGlynn, Morphological control of ZnO nanostructures on silicon substrates. *Superlattices and Microstructures* 42 (2007) 337-342.
- [2] G. Sberveglieri, C. Barrato, E. Comini, G. Faglia, M. Ferroni, A. Ponzani, A. Vomiero, Synthesis and characterization of semiconducting nanowires for gas sensing. *Sens. Actuators, B, Chem* 121 (2007) 208-213.
- [3] R. Rella, P. Siciliano, S. Capone, M. Epifani, L. Vasanelli, A. Licciulli, Air Quality Monitoring by Means of Sol-Gel Integrated Tin Oxide Thin Films. *Sens. Actuators, B*, 58 (1999) 283-288.
- [4] N. Yamazoe, K. Shimano, Roles of shape and size of component crystals in semiconductor gas sensors in response to oxygen, *J. Electrochem. Soc.*, 155, 4 (2008) J85-J92
- [5] L.J. Bie, X.N. Yan, J. Yin, Y.Q. Duan, Z.H. Yuan, Nanopillar ZnO gas sensor for hydrogen and ethanol. *Sens. Actuators, B, Chem* 126 (2007) 604–608.
- [6] F. Chaabouni, M. Abaab, B. Rezig, Metrological characterization of ZnO oxygen sensor at room temperature. *Sens. Actuators, B, Chem* 100 (2004) 200-204.
- [7] E. Comini, C. Baratto, C. Faglia, M. Ferroni, G. Sberveglieri, Single crystal ZnO nanowires as optical and conductometric chemical sensor, *J. Phys. D: Appl. Phys.* 40 (2007) 7255-7259.
- [8] C.M. Carney, S. Yoo, S.A. Akbar, TiO<sub>2</sub> - SnO<sub>2</sub> nanostructures and their H<sub>2</sub> sensing behavior, *Sens. Actuators, B, Chem* 108 (2005) 29-33.
- [9] P. Ghouma, K. Kalyanasundaram, A. Bishop, Electrospun single-crystal MoO<sub>3</sub> nanowires for biochemistry sensing probes, *J. Mat. Res.* 21, 11 (2006) 2904-2910.
- [10] K. Buchholt, E. Ieva, L. Torsi, N. Cioffi, L. Colaianni, F. Söderlind, P.O. Käll, A. Lloyd Spetz, Electrochemically synthesized Pd- and Au-nanoparticles as sensing layers in NO<sub>x</sub>-sensitive Field

Effect Devices, in S.C. Mukhopadhyay, G.S. Gupta (Eds), Smart Sensors and Sensing Technology, Springer, Berlin Heidelberg, Germany, vol. 20, 2008, pp.63-76 (ISBN: 978-3-540-79589-6).

[11] C. Di Natale, R. Paolesse, A. D'Amico, Metalloporphyrins based artificial olfactory receptors, *Sens. Actuators, B, Chem* 121 (2007) 238-246

[12] I. Lundström, H. Sundgren, F. Winqvist, M. Eriksson, C. Krantz-Rülcker, A. Lloyd Spetz, Twenty-five years of field effect gas sensor research in Linköping. *Sens. Actuators, B, Chem* 121 (2007) 247-262.

[13] M. Wallin, H. Grönbeck, A. Lloyd Spetz, M. Skoglundh, Vibrational study of ammonia adsorption on Pt/SiO<sub>2</sub>. *Appl Surf Sci* 235 (2004) 487-500.

[14] R. Yakimova, G. Steinhoff, R.M. Petoral Jr., C. Vahlberg, V. Khranovskyy, G.R. Yazdi, K. Uvdal, A. Lloyd Spetz, Novel material concepts of transducers for chemical and biosensors, *Biosensors and Bioelectronics* 22 (2007) 2780–2785.

[15] R.M. Petoral Jr., G.R. Yazdi, A. Lloyd-Spez, R. Yakimova, K. Uvdal, Organosilane-functionalized wide bandgap semiconductor surfaces. *Appl. Phys. Lett.* 90 (2007) 223904-1-223904-3.

[16] V. Khranovskyy, U. Grossner, O. Nilsen, V. Lazorenko, G.V. Lashkarev, B.G. Svensson, R. Yakimova, Structural and morphological properties of ZnO:Ga thin films. *Thin Solid Films* 515, 2, (2006) 472-476.

[17] V. Khranovskyy, R. Minikayev, S. Trushkin, G. Lashkarev, V. Lazorenko, U. Grossner, W. Paszkowicz, A. Suchocki, B.G. Svensson, R. Yakimova, Improvement of ZnO thin film properties by application of ZnO buffer layers. *Journal of Crystal Growth* 308, 1, (2007) 93-98.

[18] V. Khranovskyy, A. Ulyashin, G. Lashkarev, B.G. Svensson, R. Yakimova, Morphology, electrical and optical properties of undoped ZnO layers deposited on silicon substrates by PEMOCVD. *Thin Solid Films* 516, 7 (2008) 1396-1400.

- [19] V. Khranovskyy, U. Grossner, V. Lazorenko, G. Lashkarev, B.G. Svensson, R. Yakimova, PEMOCVD of ZnO thin films, doped by Ga and some of their properties. *Superlattices and Microstructures* 39 (2006) 275-281.
- [20] M. Berber, V. Bulto, R. Kliß, H. Hahn, Transparent nanocrystalline ZnO films prepared by spin coating. *Scripta Materialia* 53 (2005) 547-551.
- [21] A. D'Amico, C. Di Natale, Contribution on some basic definitions of sensors properties. *IEEE Sensors J.* 1 (2001) 183-190.
- [22] D.H. Yoon, G.M. Choi, Microstructure and CO gas sensing properties of porous ZnO produced by starch addition. *Sens. Actuators, B, Chem* 45 (1997) 251-257.
- [23] J.H. Yu, G.M. Choi, Electrical and CO gas sensing properties of ZnO–SnO<sub>2</sub> composites. *Sens. Actuators, B, Chem* 52 (1998) 251-256.
- [24] A. Dierstein, H. Natter, F. Meyer, H.O. Stephan, C. Kropf, R. Hempelmann, Electrochemical deposition under oxidizing conditions (EDOC): a new synthesis for nanocrystalline metal oxides. *Scripta Materialia* 44 (2001) 2209-2212.
- [25] H. Natter, R. Hempelmann, Tailor-made nanomaterials designed by electrochemical methods. *Electrochimica Acta* 49 (2003) 51-61.
- [26] N. Jayadev Dayan, S.R. Sainkar, R.N. Karekar, R.C. Aiyer, Formulation and characterization of ZnO:Sb thick-film gas sensors. *Thin Solid Films* 325 (1998) 254-258.
- [27] N. Yamazoe, K. Shimano, Theory of power laws for semiconductor gas sensors, *Sens. Actuators, B, Chem.* 128 (2008) 566-573.
- [28] D. Koziej, K. Thomas, N. Barsan, F. Thibault-Starzyk, U. Weimar, Influence of annealing temperature on the CO sensing mechanism for tin dioxide based sensors, – Operando studies. *Catalysis Today* 126 (2007) 211-218.

[29] A. Lloyd Spetz, J. Eriksson, S. Ehrler, V. Khranovskyy, R. Yakimova, P.O. Käll, Gas sensors based on ZnO nanoparticles or film: A comparison, Proc. IMCS 12, Columbus, OHIO, USA, July 13-16, 2008, pp. 489-490.

## Biographies

*Jens Eriksson* has an MSc in Electrical Engineering (received in 2005) and a BsC in Physics (received in 2006) from Linköping University, Sweden. After receiving his degrees he joined the Swedish Sensor Centre (S-SENCE), working with the development of chemical sensors based on MOS structures and the characterization of sensing layers. Since September 2007, he is working as a Marie Curie early stage researcher at CNR-IMM in Catania, focusing on the study of physical aspects related to device fabrication processes in 3C-SiC grown on hexagonal SiC substrates.

*Volodymyr Khranovskyy* graduated from the Department of Physical Electronics of Chernivtsi National University in Ukraine in 2001. As a PhD student at the Institute for Problems of Material Sciences, Ukrainian Academy of Sciences, his area of interest has been ZnO MOCVD growth and characterization. Starting from 2007 he is a visiting researcher at the IFM of Linköping University, Sweden and deals with growth of low-dimensional ZnO objects and their characterization in terms of application in optoelectronics, sensor technique etc. His activity is mainly within the VINN Excellence centre, FunMat, Functional Nanostructured Materials as well as within ZnO projects supported by the Swedish Institute.

*Fredrik Söderlind* is born 1971 and took his Master degree in chemistry and mathematics at Linköping University (Sweden) in 2001. He became PhD in chemistry in June 2008 at the same university. His main interest is inorganic synthesis, in particular of nanosized materials. In characterising the materials he uses TEM, SEM, XRD and FT-IR. At present he is an employee at Beakon Technologies AB in Malmö, Sweden.

*Per-Olov Käll* received his PhD in inorganic chemistry in 1991 at Stockholm University and since 1996 he is Assoc. Prof. at the Dept. of Physics, Chemistry and Biology at Linköping University, Sweden. His main interests lay within the fields of materials and structural chemistry and in recent years he has been mainly occupied by the chemical synthesis of nanosized materials. He is member of the board of The Centre in Nano science and technology (CeNano) at Linköping University.

*Rositza Yakimova* is professor in material science, Linköping University (LiU), in the field of semiconductor physics and technology. She has today 35 years of experience in growth and characterization of semiconductor materials, such as SiC, AlN, ZnO, etc. She is an internationally recognized expert in this field and she has been invited to several universities to share her competence. Since 1993 she has had a leading role in the development of the sublimation growth process of SiC crystals at LiU. The first SiC sublimation growth reactors in Sweden were designed with her essential contribution in collaboration with Aixtron AB-Sweden. During 1995-1999 she was employed by the company Okmetic, which preceded Norstel. In the recent years she participated in a technology transfer, as a consultant of Aixtron (former Epigress). She has done pioneered research and excellent results in AlN

crystal growth and fabrication of large area homogeneous graphene and single crystal graphite on SiC. In 2004 Yakimova was awarded a prestigious Senior Individual Grant by SSF.

*Anita Lloyd Spetz* received her PhD in 1989 at the Laboratory of Applied Physics in Linköping. From 2004 she is appointed Professor in Sensor Science, especially Chemical Sensors. From 1995-2006 she has been working as a project leader at S-SENCE, Swedish Sensor Centre (centre of excellence). From 2007 she is the Vice Director of the VINN Excellence centre, FunMat, Functional nanostructured Materials. Her research group works on development, sensing mechanism and applications of silicon carbide based field effect high temperature sensors. She is also involved in the development of resonator sensors. The applications are performed in projects together with industry (Volvo Technological Development, Volvo Cars, Ford Innovation Center, Norstel, SKF-ERC, ZnOrdic). She is also involved in the start up of a spin off company, SenSiC AB, for commercialisation of silicon carbide based field effect gas sensors. Anita Lloyd Spetz has published more than 130 papers in scientific journals and referenced conference proceedings, 9 book chapters and she has 5 patents.